

# Escaping kinetic traps using non-reciprocal interactions

Saeed Osat,<sup>1,\*</sup> Jakob Metson,<sup>1</sup> Mehran Kardar,<sup>2</sup> and Ramin Golestanian<sup>1,3,†</sup>

<sup>1</sup>*Max Planck Institute for Dynamics and Self-Organization (MPI-DS), 37077 Göttingen, Germany*

<sup>2</sup>*Department of Physics, Massachusetts Institute of Technology, Cambridge, MA 02139, United States*

<sup>3</sup>*Rudolf Peierls Centre for Theoretical Physics, University of Oxford, Oxford OX1 3PU, United Kingdom*

(Dated: September 4, 2023)

Kinetic traps are a notorious problem in equilibrium statistical mechanics, where temperature quenches ultimately fail to bring the system to low energy configurations. Using multifarious self-assembly as a model system, we introduce a mechanism to escape kinetic traps by utilizing non-reciprocal interactions between components. Introducing non-equilibrium effects offered by broken action-reaction symmetry in the system, we can push the trajectory of the system out of arrested dynamics. The dynamics of the model is studied using tools from the physics of interfaces and defects. Our proposal can find applications in self-assembly, glassy systems and systems with arrested dynamics.

Since the pioneering work of H.A. Kramers [1], studies of activated barrier crossing have found applications in a variety of situations where systems are trapped in meta-stable states, such as the stripe patterns observed in the Ising model [2] and the coarsening dynamics of non-conserved Ginzburg-Landau equation [3]. Escaping from such kinetic traps at equilibrium is typically mediated by rare nucleation events of the stable phase [4], while exerting external stresses (at the boundaries) that drive the system away from equilibrium can also facilitate such transitions [5]. It is known that some biological systems with intrinsic non-equilibrium activity such as enzymes are equipped with physical mechanisms that are able to effectively lower the barrier and facilitate escape [6]. While this is an intrinsic feature for each enzyme as perfected through evolution, it is possible to shed light on how such a phenomenon could emerge through mechanochemical coupling of such molecular oscillators with stochastic barrier-crossing dynamics [7, 8]. In light of this observation, it will be interesting to pose the following general question: how can we design non-equilibrium strategies for systems with many interacting degrees of freedom that can enable them to collectively overcome kinetic barriers using local free energy input? Here, we present a strategy to achieve this goal by utilizing the recently developed concept of non-reciprocal interactions in active matter as implemented to trigger dynamic shape-shifting in self-assembled structures [9].

Kinetic traps, also known as *chimeric traps* in the context of self-assembly, present a significant challenge in the field of equilibrium self-assembly [10]. Self-assembly involves the aggregation of small building blocks to create larger structures with desired shapes and functions [11–13]. The design problem in self-assembly entails constructing an interaction matrix, which specifies the connectivity between tiles to achieve the desired final configuration [14, 15]. However, this specificity alone does not guarantee error-free self-assembly, even at low temperatures [10], as can for example be seen in the context of the so-called multifarious self-assembly (MSA) model

[16]. The promiscuity of the tiles and their cross-talk can lead to scenarios where partially incomplete patterns assemble to form chimeras, which are analogous to the long-lived metastable states observed in spin models [16, 17].

Non-reciprocal interactions, where the action-reaction symmetry is broken, have found applications in many areas of active matter physics [18–27]. In the context of self-assembly, the non-reciprocal multifarious self-organization (NRMSO) model [9] that incorporates non-reciprocal interactions exhibits a unique dynamical feature where a self-assembled structure can switch between different predefined configurations. We demonstrate that non-reciprocal interactions enable self-assembly systems to escape metastable states that would otherwise persist for a long time in equilibrium conditions. This escape mechanism involves either the roughening of a line defect or a combination of roughening and the dynamics of point defects.

*Chimeric kinetic traps in MSA.*—We begin by setting out the concrete framework in which we study the problem of kinetic trap escape in the context of the equilibrium MSA model, which consists of a shared pool of tiles and an interaction matrix that specifies the interactions between these tiles. This system is designed to store a diverse set of predefined target structures using the available tiles in the shared pool [16, 28, 29]. The design rule employed in this model encodes these structures in the interaction matrix, effectively turning the pool into an associative memory, reminiscent of a Hopfield network [30, 31]. This associative memory is capable of retrieving individual stored target structures, analogous to the patterns settling on the energy minima in the Hopfield model. To successfully retrieve a pattern in MSA, it is necessary to initiate the process close to the corresponding energy minimum, which can be achieved by introducing a small seed of the pattern, or by employing concentration patterning techniques [16, 32]. However, as more patterns are stored in the system the increased cross-talk between tiles leads to the formation of many local minima corresponding to spurious pat-

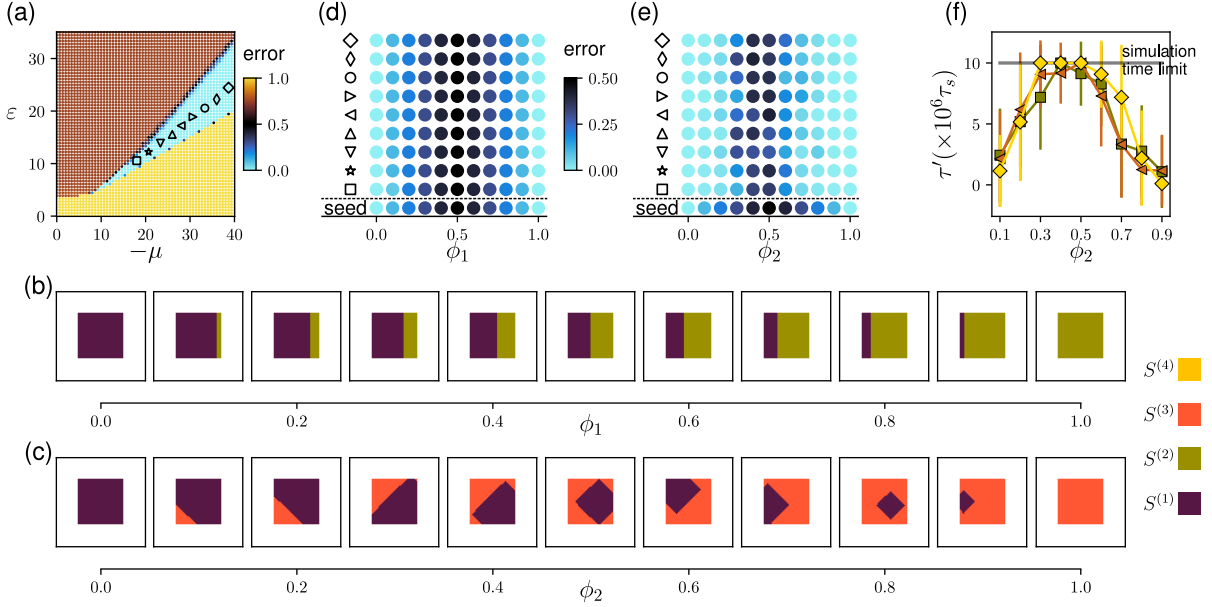


FIG. 1. Chimeric kinetic traps. Four desired patterns of size  $40 \times 40$  are made of random permutations of 1600 distinct tiles and are colored uniquely. Panel (a) displays the  $(\epsilon - \mu)$  state diagram of the MSA model, with the cyan region indicating the regime of robust self-assembly. Panels (b) and (c) present synthetic chimeric seeds used in the simulations, created by combining two desired patterns. In panel (b), the type 1 seeds exhibit smooth boundaries and are energetically stable, while in panel (c), the type 2 seeds display jagged boundaries.  $\phi_1$  and  $\phi_2$  characterize the composition of the type 1 and type 2 chimeric seeds respectively, where extreme values (0 and 1) indicate seeds composed solely of one of the desired patterns. Panel (d) illustrates the average error over 10 independent realizations when starting from seeds of type one, revealing that the system becomes strongly trapped in the initial configuration. Similarly, panel (e) shows the average error when starting from seeds of type two. Seeds close to  $\phi_2 = 0$  and  $\phi_2 = 1$  are absorbed into basins of attraction corresponding to the target patterns, while seeds with  $\phi_2 \approx 0.5$  remain kinetically trapped. Panel (f) demonstrates the first passage time to the nearest error-free configuration plotted against  $\phi_2$ , confirming the absorption of trajectories towards the target patterns. The different markers correspond to three representative points in the error-free MSA regime.

terns [33], which is analogous to exceeding the capacity of the Hopfield model. Since the pool is shared, each tile is involved in interactions with different neighboring tiles in each structure, leading to a promiscuous behavior of the tiles [34].

We consider  $m = 4$  desired target structures, each of which is a random permutation of  $M = 40 \times 40$  distinct tiles arranged in a 2D square lattice with a side length of  $\sqrt{M} = 40$ . The design rule of self-assembly is as follows: two tiles interact specifically with an interaction strength  $\epsilon$  if they are adjacent in at least one of the desired patterns. We use a grand canonical ensemble, in which all of the tiles have the same chemical potential  $\mu$ , except for empty lattice points. The simulation system is a square lattice with a side length of  $2 \times \sqrt{M}$ , and the initial seed is placed at the center of the system (see the Supplemental Material and Ref. [9] for details of the model). Figure 1(a) shows the error of self-assembly in the  $(\epsilon, \mu)$  parameter space when starting with the whole pattern as the initial seed. As is common in self-assembly models, the MSA model suffers from a high-dimensional parameter space where only a small fraction of the parameter

space allows for error-free self-assembly. To investigate metastability in this model we define two different types of chimeric seeds, where two patterns are separated by a boundary that can be either commensurate with the lattice structure (type 1 chimera) or not (type 2 chimera), as shown in Fig. 1(b) and (c). Initially, a fraction  $\phi_1$  ( $\phi_2$ ) of the seed is assigned to one pattern and a fraction  $1 - \phi_1$  ( $1 - \phi_2$ ) to another pattern. We probe the behavior of the system starting from these seeds and choosing the values of  $(\epsilon, \mu)$  within the error-free region of the MSA model. If the dynamics of the system changes the initial seed to a completely assembled single pattern, then it is considered an escape from the kinetic trap; otherwise, the dynamics is arrested in the chimeric state. Figure 1(d) shows the error of self-assembly, starting from type 1 chimeras as the initial seed, for different  $(\epsilon, \mu)$  coordinates as marked in panel (a). As expected, smooth boundaries are robust, and the system cannot escape from this type of chimera, even for values of  $\phi_1$  close to 0 or 1. On the other hand, Fig. 1(e) shows the same simulations, but where the system is initialized with type 2 chimeras as the initial seed. The rugged interface shape facilitates the dynamics of

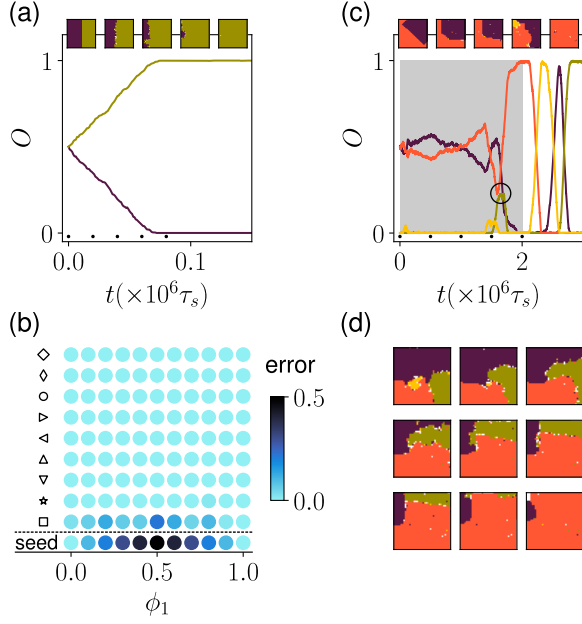


FIG. 2. Escaping kinetic traps. (a) A synthetic chimera seed made of two patterns that are encoded via non-reciprocal interactions as a sequence of length one  $S^1 \rightarrow S^2$ . The green pattern ( $S^2$ ) moves into the purple pattern ( $S^1$ ) and the system can escape the kinetic trap. The overlap  $O$  is the fraction of the system filled by each pattern. The black dots on the time axis mark the times of the snapshots. (b) Error of the final configuration for type 1 chimera when non-reciprocal interactions are deployed. (c) A chimera made of non-consecutive patterns  $S^1$  and  $S^3$  in a cyclic sequence  $S^1 \rightarrow S^2 \rightarrow S^3 \rightarrow S^4 \rightarrow S^1$ . Pattern  $S^3$  cannot start the shift and a nucleation of pattern  $S^2(S^4)$  within pattern  $S^1(S^3)$  is required. As soon as pattern  $S^2$  emerges, fast defect-like dynamics of the three patterns ushers the system out of the kinetic trap, as shown in (d).

chimeras and for both small and large  $\phi_2$ , the trajectory of the system is absorbed into the closest global minimum (fully assembled target pattern). However, for medium values of  $\phi_2$ , where the chimera is made up of almost equal proportions of the two structures, the dynamics is usually trapped in an alternate chimeric state (despite the smoothing of the rugged interfaces) or occasionally in blinker states [35]. Note that MSA not only stores different structures as energy minima, but it also provides basins around these minima, as we have seen in Fig. 1(e). Chimeras close to the original patterns can reach the original patterns, and require less time to do so the closer they are. This can be seen from the first passage time  $\tau'$  of reaching the error-free state for different values of  $\phi_2$ , as plotted in Fig. 1(f).

*Non-reciprocal interactions.*—The behavior of the system changes drastically in the NRMSO model in which the tiles are equipped with non-reciprocal specific interactions, which drive the system out of equilibrium with

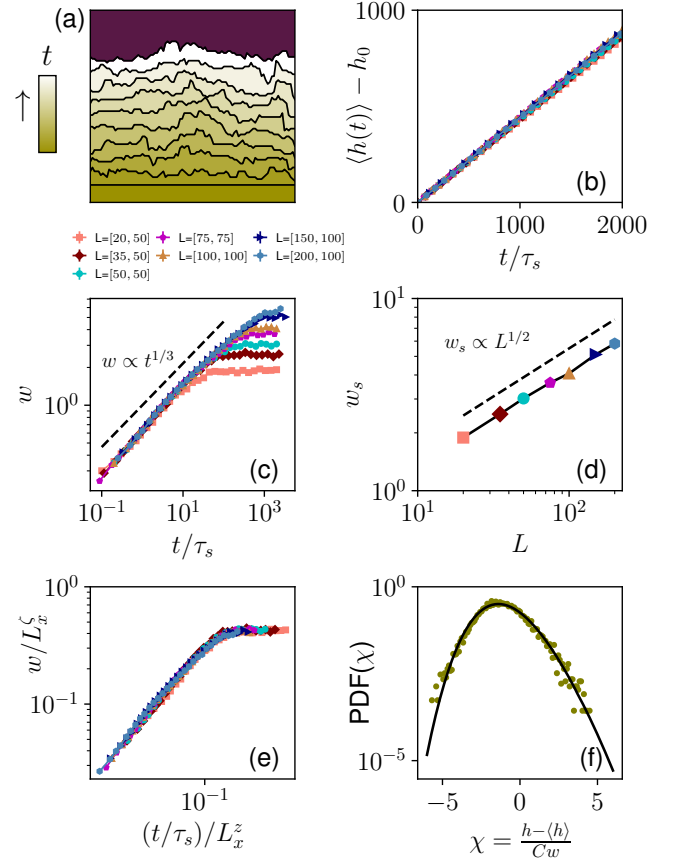


FIG. 3. Interface roughening in chimeras. Panel (a) illustrates a chimera of consecutive patterns in a sequence of length one ( $S^1 \rightarrow S^2$ ) with a smooth boundary in the seed. Panel (b) displays the average height of the interface. The velocity of the interface remains constant across different system sizes. Panel (c) demonstrates the interface roughness as a function of time, exhibiting a generic roughening regime with a growth exponent of  $\beta = 1/3$ , followed by a crossover to a saturation regime. Panel (d) shows the (saturation) roughness as a function of system size, indicating a roughness exponent of  $\zeta = 1/2$ . Panel (e) presents the scaling and collapse of the data for different system sizes with roughness exponent  $\zeta = 1/2$  and dynamic exponent  $z = 3/2$ . Panel (f) depicts the density distribution of re-scaled height fluctuations  $\chi = (h - \langle h \rangle)/(Cw)$  (where  $C$  is a fitting parameter; here  $C = 0.9$ ) and the corresponding GOE Tracy-Widom distribution for a system size of  $100 \times 100$  in the saturation regime.

local energy input [9]. As in the case of the MSA model, the strength of reciprocal interactions is  $\varepsilon$ , while the strength of non-reciprocal interactions is controlled by  $\lambda$ . For  $\frac{2}{3}\varepsilon \lesssim \lambda \lesssim \varepsilon$  robust shape-shifting behavior is observed [9] (for details of the model see the Supplemental Material).

We now demonstrate how tiles with non-reciprocal interactions can escape from the different chimeric traps introduced in Figs. 1(b) and (c). Through extensive sim-

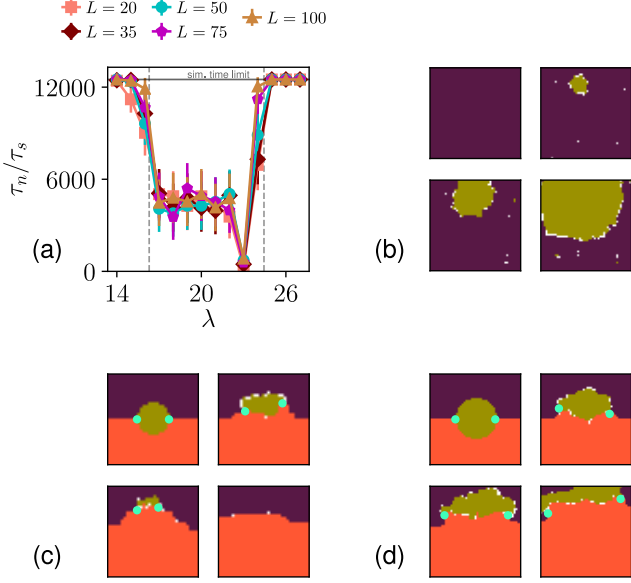


FIG. 4. Defect-mediated escape. (a) Nucleation time of  $S^2$  in a system filled with  $S^1$  rescaled by  $\tau_s$  versus  $\lambda$ , with the sequence  $S^1 \rightarrow S^2$ . Dotted vertical lines mark  $\lambda = \frac{2}{3}\epsilon$  and  $\lambda = \epsilon$ . (b) Nucleation of  $S^2$  in a sea of  $S^1$ , with sequence  $S^1 \rightarrow S^2$ . (c), (d) The system is initialised with an  $S^2$  droplet sitting on an interface between  $S^1$  and  $S^3$ , with shifting sequence  $S^1 \rightarrow S^2 \rightarrow S^3 \rightarrow S^4 \rightarrow S^1$ . Light blue dots mark where the regions of  $S^1, S^2, S^3$  meet. The full videos of (b), (c) and (d) are included as Supplemental Videos 4, 5, and 6, respectively.

ulations, we have observed two different mechanisms by which NRMSO drives the dynamics of the system out of an arrested state. The specific mechanism responsible for escaping the kinetic trap depends on the sequence of the transitions induced by interactions.

We observe that for a sequence of  $S^1 \rightarrow S^2$  a chimeric seed will start to expand the  $S^2$  region at the expense of diminishing the  $S^1$  region, as shown in Fig. 2(a). Figure 2(b) presents the same simulation as Fig. 1(d), but with tiles also exhibiting non-reciprocal interactions. All of the chimeric seeds escape the kinetic trap and are absorbed into the final state of the dynamics, a fully assembled  $S^2$  pattern. In this example, interface roughening is the mechanism of escape (see below).

Now consider the sequence  $S^1 \rightarrow S^2 \rightarrow S^3 \rightarrow S^4 \rightarrow S^1$  and a chimeric seed composed of  $S^1$  and  $S^3$ . Since there is no direct route in the sequence from  $S^1$  to  $S^3$ , a different mechanism provides a route to escaping this trap: defect nucleation. The sequence implies that there is a shape-shifting structure starting from  $S^1$  that shifts to  $S^2$ , then to  $S^3$  and  $S^4$ , and finally returns back to  $S^1$ . A shift starts when a stable seed of pattern  $S^2$  ( $S^4$ ) is nucleated within  $S^1$  ( $S^3$ ). The shift then happens much faster than nucleation, as shown in Fig. 2(c). When the nucleated  $S^2$  reaches the  $S^1 - S^3$  boundary, a defect is formed,

which starts to rotate since  $S^2$  chases  $S^1$  and  $S^3$  chases  $S^2$ , as illustrated in Fig. 2(d). From here, the system can escape to a fully assembled pattern. We will investigate both of these mechanisms of escape in more depth in the following sections.

*Interface roughening.*—Chimeras with a smooth boundary are well-suited for studying interface dynamics as they provide a smooth initial condition for interface growth. In our case, two structures ( $S^1$  and  $S^2$ ) are stored in the pool, with a shifting sequence  $S^1 \rightarrow S^2$ . Starting from a type 1 chimera, which consists of two slabs of  $S^1$  and  $S^2$ , and choosing a suitable  $\lambda$  value, the interface begins to grow, as depicted in Fig. 3(a). Since the interface moves at a constant velocity, due to a finite system size we quickly reach a system filled with  $S^2$ . Since there can be no interface without any  $S^1$  present, interface roughening and roughness saturation are no longer observed.

We can study the dynamics of this moving interface by employing a two-phase method that overcomes the limitation of finite life time (see supplemental Material for details) [36]. Videos of such simulations for different values of  $\lambda$  are shown in Supplemental Video 1. Simulations on a rectangular lattice with a height much larger than its width confirm the same results obtained using the two-phase method. Supplemental Video 2 shows a simulation with  $L_y \gg L_x$ . Figure 3(b) demonstrates that the interface moves with a constant velocity, and that this velocity remains nearly constant for all system sizes. (Videos of interface dynamics for different system sizes are given in Supplemental Video 3.) Note that  $t$  is rescaled to  $t/\tau_s$ , where  $\tau_s = (L_x \times L_y)$ . Figure 3(c) displays the roughness of the interface, defined as  $w(t) = \sqrt{\langle (h(x,t) - \langle h(x,t) \rangle_x)^2 \rangle_x}$ , for different system sizes. All the curves exhibit an initial growth exponent of  $\beta = 1/3$ , followed by a crossover to a saturation regime with a size-dependent value of  $w_s(L)$ . The saturated roughness increases with system size as  $w_s \propto L_x^\zeta$ , with a roughness exponent of  $\zeta = 1/2$ , as shown in Fig. 2(d). These exponents suggest a Kardar-Parisi-Zhang (KPZ) universality (corresponding with a dynamic exponent  $z = 3/2$ ) [37, 38]. Figure 3(e) further confirms the KPZ universality through scaling and collapse of the curves for different system sizes. Additionally, the probability density of height fluctuations follows the Gaussian orthogonal ensemble (GOE) Tracy-Widom distribution [39] as shown in Fig. 3(f), as expected from the KPZ universality class [40, 41].

*Defect nucleation.*—The second mechanism of escaping chimeric traps is via defect nucleation. This occurs when the system is trapped in a meta-stable configuration where there is no direct route for the interface to grow, as demonstrated in Figs. 2(c) and 2(d). With a sequence like  $S^1 \rightarrow S^2 \rightarrow S^3 \rightarrow S^4 \rightarrow S^1$ , the escape from a seed composed of  $S^1$  and  $S^3$  can proceed via an initial nucleation of a droplet of  $S^2$  within the  $S^1$  region



or of a droplet of  $S^4$  in  $S^3$ . To measure nucleation times, we design a sequence  $S^1 \rightarrow S^2$ , and, starting from a system filled with  $S^1$ , define the nucleation time  $\tau_n$  as the first passage time (in units of  $\tau_s$ ) of reaching  $O_2 = 0.25$ , where  $O_2$  is the overlap of the system configuration with pattern  $S^2$ . An example of a nucleation event is shown in Fig. 4(b) and Supplemental Video 4. Figure 4(a) shows  $\tau_n$  rescaled by  $\tau_s$  for different system sizes, confirming previous results on the functional region  $\frac{2}{3}\varepsilon \lesssim \lambda \lesssim \varepsilon$  where shifting occurs.

A droplet of  $S^2$  placed on the boundary of an  $S^1$ - $S^3$  chimera corresponds to two defects, as shown in Figs. 4(c) and 4(d). A small droplet can be destroyed by the chasing  $S^3$  pattern, ultimately leading to the disappearance of the point defects, which leaves the system trapped in a chimeric state, as shown in Fig. 4(c) and Supplemental Video 5. For larger droplets, the point defects repel each other and drive the system out of the chimeric trap, which can be seen in Fig. 4(d) and Supplemental Video 6.

*Conclusion.*— We introduced a method to escape kinetic traps in self-assembly using non-reciprocal interactions between the building blocks. Dynamics of the escape is quantified using tools from the physics of interfaces and defects. Our findings are general and are applicable to a diverse range of systems with arrested dynamics such as glassy systems [42, 43].

We acknowledge support from the Max Planck School Matter to Life and the MaxSynBio Consortium which are jointly funded by the Federal Ministry of Education and Research (BMBF) of Germany and the Max Planck Society.

---

\* saeed.osat@ds.mpg.de

† ramin.golestanian@ds.mpg.de

- [1] H. Kramers, Brownian motion in a field of force and the diffusion model of chemical reactions, *Physica* **7**, 284 (1940).
- [2] J. Olejarz, P. L. Krapivsky, and S. Redner, Fate of 2d kinetic ferromagnets and critical percolation crossing probabilities, *Phys. Rev. Lett.* **109**, 195702 (2012).
- [3] A. Bray, Theory of phase-ordering kinetics, *Advances in Physics* **43**, 357 (1994).
- [4] K. Binder, Theory of first-order phase transitions, *Reports on Progress in Physics* **50**, 783 (1987).
- [5] A. Zaccane, *Theory of Disordered Solids* (Springer International Publishing, 2023).
- [6] R. Golestanian, Phoretic Active Matter, in *Active Matter and Nonequilibrium Statistical Physics: Lecture Notes of the Les Houches Summer School: Volume 112, September 2018* (Oxford University Press, 2022).
- [7] J. Agudo-Canalejo, T. Adeleke-Larodo, P. Illien, and R. Golestanian, Synchronization and enhanced catalysis of mechanically coupled enzymes, *Phys. Rev. Lett.* **127**, 208103 (2021).
- [8] M. Chatzittofi, R. Golestanian, and J. Agudo-Canalejo, Collective synchronization of dissipatively-coupled noise-activated processes, *New Journal of Physics* **10.1088/1367-2630/acf2bc** (2023).
- [9] S. Osat and R. Golestanian, Non-reciprocal multifarious self-organization, *Nature Nanotechnology* **18**, 79 (2023).
- [10] S. Whitelam and R. L. Jack, The statistical mechanics of dynamic pathways to self-assembly, *Annual Review of Physical Chemistry* **66**, 143 (2015).
- [11] S. C. Glotzer, Some assembly required, *Science* **306**, 419 (2004).
- [12] G. M. Whitesides and B. Grzybowski, Self-assembly at all scales, *Science* **295**, 2418 (2002).
- [13] Z. Zhang and S. C. Glotzer, Self-assembly of patchy particles, *Nano Letters* **4**, 1407 (2004).
- [14] S. Hormoz and M. P. Brenner, Design principles for self-assembly with short-range interactions, *Proceedings of the National Academy of Sciences* **108**, 5193 (2011).
- [15] M. Nguyen and S. Vaikuntanathan, Design principles for nonequilibrium self-assembly, *Proceedings of the National Academy of Sciences* **113**, 14231 (2016).
- [16] A. Murugan, Z. Zeravic, M. P. Brenner, and S. Leibler, Multifarious assembly mixtures: Systems allowing retrieval of diverse stored structures, *Proceedings of the National Academy of Sciences* **112**, 54 (2015).
- [17] A. Murugan, J. Zou, and M. P. Brenner, Undesired usage and the robust self-assembly of heterogeneous structures, *Nature Communications* **6**, 6203 (2015).
- [18] N. Uchida and R. Golestanian, Synchronization and collective dynamics in a carpet of microfluidic rotors, *Phys. Rev. Lett.* **104**, 178103 (2010).
- [19] R. Soto and R. Golestanian, Self-assembly of catalytically active colloidal molecules: Tailoring activity through surface chemistry, *Phys. Rev. Lett.* **112**, 068301 (2014).
- [20] A. V. Ivlev, J. Bartnick, M. Heinen, C.-R. Du, V. Nosenko, and H. Löwen, Statistical Mechanics where Newton's Third Law is Broken, *Phys. Rev. X* **5**, 011035 (2015).
- [21] J. Agudo-Canalejo and R. Golestanian, Active phase separation in mixtures of chemically interacting particles, *Phys. Rev. Lett.* **123**, 018101 (2019).
- [22] S. Saha, J. Agudo-Canalejo, and R. Golestanian, Scalar active mixtures: The nonreciprocal cahn-hilliard model, *Phys. Rev. X* **10**, 041009 (2020).
- [23] S. A. M. Loos and S. H. L. Klapp, Irreversibility, heat and information flows induced by non-reciprocal interactions, *New Journal of Physics* **22**, 123051 (2020).
- [24] Z. You, A. Baskaran, and M. C. Marchetti, Nonreciprocity as a generic route to traveling states, *Proceedings of the National Academy of Sciences* **117**, 19767 (2020).
- [25] A. Dinelli, J. O'Byrne, A. Curatolo, Y. Zhao, P. Sollich, and J. Tailleur, *Non-reciprocity across scales in active mixtures* (2022).
- [26] S. A. M. Loos, S. H. L. Klapp, and T. Martynek, Long-range order and directional defect propagation in the nonreciprocal XY model with vision cone interactions, *Phys. Rev. Lett.* **130**, 198301 (2023).
- [27] V. Ouazan-Reboul, J. Agudo-Canalejo, and R. Golestanian, Self-organization of primitive metabolic cycles due to non-reciprocal interactions, *Nature Communications* **14**, 10.1038/s41467-023-40241-w (2023).
- [28] P. Sartori and S. Leibler, Lessons from equilibrium statistical physics regarding the assembly of protein complexes, *Proceedings of the National Academy of Sciences* **117**, 114 (2020).

- [29] G. Bisker and J. L. England, Nonequilibrium associative retrieval of multiple stored self-assembly targets, *Proceedings of the National Academy of Sciences* **115**, E10531 (2018).
- [30] J. J. Hopfield, Neural networks and physical systems with emergent collective computational abilities, *Proceedings of the National Academy of Sciences* **79**, 2554 (1982).
- [31] D. J. Amit, H. Gutfreund, and H. Sompolinsky, Storing infinite numbers of patterns in a spin-glass model of neural networks, *Phys. Rev. Lett.* **55**, 1530 (1985).
- [32] C. G. Evans, J. O'Brien, E. Winfree, and A. Murugan, Pattern recognition in the nucleation kinetics of non-equilibrium self-assembly (2022), [arXiv:2207.06399 \[cond-mat.dis-nn\]](https://arxiv.org/abs/2207.06399).
- [33] D. J. Amit, H. Gutfreund, and H. Sompolinsky, Spin-glass models of neural networks, *Phys. Rev. A* **32**, 1007 (1985).
- [34] M. H. Huntley, A. Murugan, and M. P. Brenner, Information capacity of specific interactions, *Proceedings of the National Academy of Sciences* **113**, 5841 (2016).
- [35] J. Olejarz, P. L. Krapivsky, and S. Redner, Zero-temperature coarsening in the 2d potts model, *Journal of Statistical Mechanics: Theory and Experiment* **2013**, P06018 (2013).
- [36] P. Devillard and H. Spohn, Kinetic shape of ising clusters, *Europhysics Letters* **17**, 113 (1992).
- [37] M. Kardar, G. Parisi, and Y.-C. Zhang, Dynamic scaling of growing interfaces, *Phys. Rev. Lett.* **56**, 889 (1986).
- [38] A.-L. Barabási and H. E. Stanley, *Fractal Concepts in Surface Growth* (Cambridge University Press, 1995).
- [39] C. A. Tracy and H. Widom, On orthogonal and symplectic matrix ensembles, *Communications in Mathematical Physics* **177**, 727 (1996).
- [40] I. Corwin, The kardar–parisi–zhang equation and universality class, *Random Matrices: Theory and Applications* **01**, 1130001 (2012).
- [41] K. A. Takeuchi and M. Sano, Universal fluctuations of growing interfaces: Evidence in turbulent liquid crystals, *Phys. Rev. Lett.* **104**, 230601 (2010).
- [42] T. R. Kirkpatrick and P. G. Wolynes, Stable and metastable states in mean-field potts and structural glasses, *Phys. Rev. B* **36**, 8552 (1987).
- [43] G. Parisi, P. Urbani, and F. Zamponi, *Theory of Simple Glasses: Exact Solutions in Infinite Dimensions* (Cambridge University Press, 2020).